Journal of Oral Pathology & Medicine

WILEY

Journal of Oral Pathology & Medicine

ORIGINAL ARTICLE OPEN ACCESS

Radiologic Specific Growth Rate of Ameloblastomas: A Clinicopathological Correlation

Chané Smit[1,2] | Liam Robinson[1] | Marlene B. van Heerden[1] | Pieter W. Meyer[3] | Felipe P. Fonseca[1,4] | Willie F. P. van Heerden[1,5] | André Uys[2]

[1]Department of Oral and Maxillofacial Pathology, Faculty of Health Sciences, University of Pretoria, Pretoria, South Africa | [2]Department of Anatomy, Faculty of Health Sciences, University of Pretoria, Pretoria, South Africa | [3]Department of Immunology, Faculty of Health Sciences, Tshwane Academic Division, University of Pretoria, National Health Laboratory Services, Pretoria, South Africa | [4]Department of Oral Surgery and Pathology, School of Dentistry, Federal University of Minas Gerais (UFMG), Belo Horizonte, Brazil | [5]PathCare Vermaak Histopathology, Pretoria, South Africa

Correspondence: Chané Smit (chane.smit@up.ac.za)

Received: 3 July 2024 | **Revised:** 18 November 2024 | **Accepted:** 1 January 2025

Funding: The authors received no specific funding for this work.

Keywords: ameloblastoma | growth | histology | proliferation | radiology

ABSTRACT

Background: The study aimed to assess the radiologic-specific growth rate of ameloblastomas, evaluating potential associations with demographics, radiologic features, histopathologic variants and proliferation indices. The results of this study will hopefully establish if any clinical or histopathologic features can elude fast-growing ameloblastomas.

Methods: Patients presenting with multiple radiographs before surgical intervention due to various healthcare constraints or patient factors were included in the study. The measurements from each radiograph included the lesion's length, height, width and amount of expansion in these dimensions. Furthermore, the circumference of the lesion was measured in sagittal, coronal and axial planes. The radiologic-specific growth rate was assessed by calculating the difference in measurements from the initial to follow-up radiographs divided by the duration between the visits to calculate the growth rate per year.

Results: The specific growth rate was analysed between age groups, histopathologic variants and Ki-67 values, with no statistically significant correlations found in all dimensions measured. A statistically significant faster growth ($p = 0.04$) was seen in females when measuring the mesial-distal length. When comparing radiologic features, ameloblastomas with loss of border demarcation, severe cortical destruction and tooth displacement demonstrated statistically significant faster growth.

Conclusion: This study found significant correlations with the growth rate of ameloblastomas, specifically in coronal dimensions, supporting the notion of buccal-lingual growth/expansion for which ameloblastomas are known.

1 | Introduction

Ameloblastoma (AB) is a benign odontogenic neoplasm of epithelial origin with aggressive biological behavior [1]. ABs arising within bone are broadly classified into unicystic and conventional variants. Unicystic ABs are subdivided into luminal, intraluminal and mural, depending on their specific growth pattern. Similarly, conventional ABs have various histopathologic subtypes, including follicular, plexiform, acanthomatous, granular, basal cell and desmoplastic. Rare histopathologic variants, including keratoameloblastoma, have also been described [2].

The aetiopathogenesis of ABs includes an initial monoclonal mutation in genes involving the mitogen-activated protein kinase (MAP-K) pathway. The *BRAF* gene is commonly implicated in ABs with less common associated mutations, including the *KRAS, NRAS, HRAS*, *FGFR2* and the hedgehog signalling pathway activating the *SMO* gene [1].

The proliferative potential of neoplastic cells provides insight into the overall biological behaviour of a tumour. Therefore, the measurement of the proliferation index via Ki-67 immunohistochemistry (IHC) gives insight into the biological aggressiveness of a tumour, being both a prognostic and predictive factor, and directing the clinical course of a disease, ultimately guiding management [3].

The growth of ABs has been a topic of interest as they exhibit aggressive patterns, reflected in the progression of their radiologic appearances over time [4, 5]. Moreover, certain subtypes of ABs behave and are treated differently, especially the subtypes of unicystic ABs. Whether a difference exists between the subtypes of conventional ABs has not been fully clarified. Some studies note important differences between the conventional subtypes, including demographics, radiologic features, Ki-67 proliferation values and recurrence rates [6–9]. However, the comparison of these parameters against tumour growth has not been assessed.

Specific growth rate (SGR), as described by Mehrara et al. [10], was initially utilised to assess tumour response to treatment by calculating the increase or decrease of tumour volume over a specific time period. This formula has been used in AB studies using clinical, radiologic and histologic measurements [11]. Furthermore, the formula has also been adapted to two-dimensional linear measurements in ABs [12].

In developing countries, various healthcare constraints or patient factors may result in a loss of patient follow-up or treatment interruption [11], resulting in multiple pre-treatment radiographs. This study aimed to assess the SGR of ABs using radiographic images, evaluating associations with demographics, radiologic features, histopathologic variants and proliferation indices. The results are expected to characterise clinical or histopathologic features that may identify fast-growing ABs.

2 | Materials and Methods

2.1 | Study Participant Selection

Histopathologically diagnosed cases of ABs were retrieved from the digital database of the Department of Oral and Maxillofacial Pathology, University of Pretoria. To meet the study objectives, included cases required initial and follow-up digital radiographs of adequate diagnostic quality in the database before definitive treatment. Furthermore, included cases needed sufficient preserved formalin-fixed paraffin-embedded tissue to confirm the diagnosis, determine the histopathologic subtype, and perform Ki-67 IHC analysis.

2.2 | Histopathological Analysis

Diagnosis confirmation, histopathologic subtyping and IHC analysis were performed on the most representative section (resection over biopsy sample) of the tumour from all available specimens for each included case. The histopathologic variant was classified based on the predominant pattern visible in all sections of the tumour, following the latest WHO classification of head and neck tumours [1]. Ki-67 IHC analysis was performed on freshly cut 3 μm sections for each included case using Ventana rabbit monoclonal Ki67 (clone 30-9) antibody. Staining was performed on a Ventana Benchmark GX Automated System (Ventana Medical Systems Inc., Tucson, Arizona, 85755 USA) according to the manufacturer's recommendations using the Ventana OptiView DAB IHC detection kit. Sections were then counterstained with haematoxylin and mounted with a permanent mounting media. Appropriate positive controls were included in all cases. The proliferation index was calculated by counting at least 100 cells at a hot spot in a representative tumour section. Areas with a dense inflammatory infiltrate were not evaluated due to the influence on the proliferation index.

2.3 | Radiologic Analysis

Demographic data was retrieved from the patient's records. Digital radiographs, including panoramic (PR) and skull radiographs, and specialised imaging, consisting of computerised tomography (CT) and cone-beam CT (CBCT), were utilised for radiological evaluation. The investigators were blinded to the histopathologic variant and proliferation index when the radiographs were assessed.

To determine the SGR of included cases, diagnostically acceptable radiographs were collected and imported to ImageJ software (National Institutes of Health), version 1.8.0, in JPG format. After this, the radiographic measurements were calibrated for magnification between each examination (initial and follow-up radiographs) per patient using the mesiodistal dimension of a tooth in proximity to the lesion (not affected or displaced by the tumour), similar to the methodology employed by Mariz et al. [12] Due to differences in imaging modalities, physical measurements were not expressed to indicate growth, rather a percentage of growth between two calibrated images per patient.

The measurements from each radiograph included the greatest diagonal dimension, length (mesial–distal), height (superior–inferior) and width (medial–lateral) dimensions of the lesion (Figure 1). These were measured using a method similar to that of a previous study by Merbold et al. [4] On two-dimensional (2D) imaging, the length was defined as the largest dimension of the lesion measured by a line running parallel to the inferior border of the mandible on a panoramic radiograph. The height was measured by a line perpendicular to the inferior border of the mandible. The width was only measurable on 2D imaging when a radiograph at a right angle to the lesion was available (e.g., a posterior–anterior skull radiograph if the lesion was located in the posterior mandible). On CBCT imaging, a panoramic radiograph was constructed from the volumetric data to measure the length and height, similar to the measurements on the panoramic radiograph. The width was measured at the widest lesion dimension on the coronal section. Additional measurements included the amount of expansion in all three dimensions, as previously mentioned, if available. This was done by comparing the size of the lesion to a contralateral reference. For example, the expansion of the ramus was compared to the normal contralateral ramus measurements (amount of expansion of the affected ramus minus the contralateral normal ramus). Furthermore, the circumference of the lesion was measured using the software

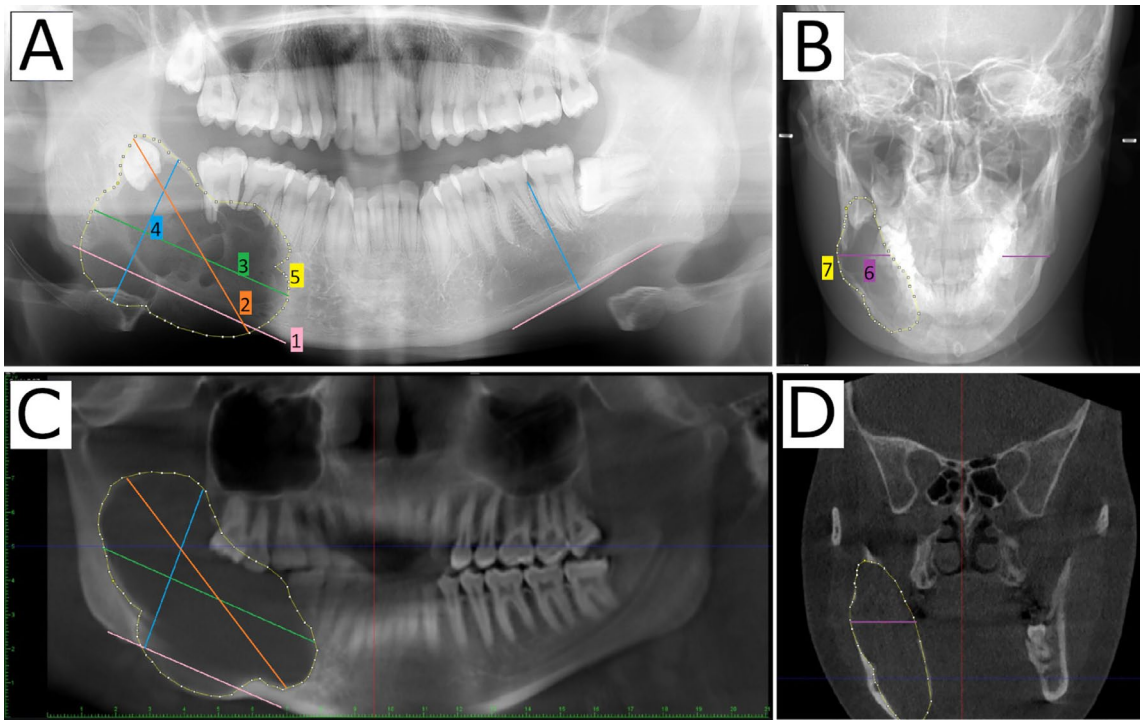

FIGURE 1 | Image measurement on 2D images (A, B). The diameter of the lesion is measured at a line corresponding to the largest overall dimension of the lesion (2). The length of the lesion (3) is measured at the widest mesial-distal dimension using a line parallel to the inferior mandibular border (1). The height of the lesion (4) is measured using a line perpendicular to the inferior mandibular border. The sagittal circumference (5) is measured using the polygon tool. The width of the lesion (6) and coronal circumference (7) is measured on skull radiographs. On CBCT images, a panoramic radiograph is reconstructed from the volumetric data and measured similarly as described above (C). The width and coronal circumference are measured on CBCT imaging in the coronal slice at the widest lesion dimensions (D).

polygon selection tool on sagittal (panoramic view), coronal and axial planes (when available) on CBCT images.

The SGR was assessed by calculating the difference in calibrated measurements from initial to follow-up radiographs divided by the duration between the visits to obtain the growth rate per year, as described by Mehrara et al. [10] where M_1 represents the initial measurement, and M_2 represents the follow-up. Similarly, T1 represents the date of the first radiograph, and T2 represents the follow-up date to calculate the duration between examinations.

$$\mathrm{SGR} = \frac{ln\,(M_2/M_1)}{T_2 - T_1}.$$

Each measurement was taken at the widest dimensions of the lesion and remeasured three times. The average of all three measurements was used. The SGR of included cases, expressed as a percentage of growth (%) between radiographs, was analysed to assess for any associations with demographics, radiologic features, histopathologic variants and proliferation indices.

2.4 | Statistical Analysis

The results of the various analyses were recorded using Microsoft Excel (Version 2016), and subsequent statistical analysis of the categorical data was performed using Stata 18.0 SE (StataCorp LLC, TX, USA). The distribution of data was confirmed using the Shapiro–Wilk test. Descriptive statistics were reported using median and interquartile ranges. Kruskal–Wallis and Dunn's pairwise comparison using rank sums with Bonferroni correction was used for multiple comparisons, including SGR and radiologic features, age, histopathologic variants and Ki-67 proliferation scores. The Wilcoxon signed-rank test was used to compare SGR with sex. Asymptotic Significance (p-value) of less than 0.05 was considered statistically significant. Intra-examiner reliability was assessed by the principal author (CS) remeasuring randomly selected cases constituting 15% of the sample 3 months later. Inter-examiner reliability was evaluated by analysing 15% of the sample by another investigator (AU) with experience in the field of Maxillofacial Radiology. This was assessed using Bland Altman and Lin's Concordance correlation coefficient.

3 | Results

Over the 11-year period (2013–2023), 54 cases met the inclusion criteria, with 54 initial and 86 follow-up radiographs (total of 140 radiographs) included in the final sample. The median age of included cases was 32.5 years, and the sample had a 1:1.2 male-to-female ratio. The median duration from the initial to last follow-up radiograph before definitive treatment was 0.73 years (mean = 1.5 years). Only 38 cases had radiologic evidence of treatment at the same institution and the median duration between initial to treatment radiograph was 1.5 years.

The radiologic SGR was analysed with age (Table 1), with the majority of fast growth seen in the fourth quartile (ages 47–76 years), although not statistically significant ($p > 0.36$). This growth was not considered a factor of time, as the duration between radiographs in this group (1.33 years) was comparable to the duration of the other age quartiles. Comparing the SGR between sexes (Table 2), a statistically significant faster SGR ($p = 0.04$) was seen in females when measuring the mesial-distal length. The length expansion and volume were also notably greater in females, although not statistically significant. Males had higher SGR rates, albeit not statistically significant, when the circumference of the lesion was measured in the coronal and axial dimensions. Interestingly, males presented at a later age (39.19 vs. 26.44 years) and a shorter duration between radiographs (0.58 vs. 0.77 years) compared with females.

The SGR of ABs was compared with various radiologic features, and the results are summarised in Table 3. A statistically significant difference was noted when comparing SGR to the borders of ABs, with faster growth in the coronal circumference seen in ABs with loss of border demarcation. However, contrary to this finding, faster SGR was generally seen in lesions with well-defined borders. In general, lesion locularity did not influence the SGR. Regarding effects on the surrounding bone, statistically significant higher SGR was noted in tumours with severe cortical destruction in the coronal dimension ($p = 0.007$). The SGR in length was significantly lower in lesions with cortical thinning versus destruction ($p = 0.02$). Effects on surrounding teeth revealed that tooth displacement was noted with significantly higher SGR in length compared to root resorption ($p = 0.002$).

When analysing the histopathologic variants of AB, the majority of cases included in the study were classified as follicular (18 cases), followed closely by acanthomatous (17 cases), granular cell (6 cases) and plexiform (5 cases) variants, with the other variants being rare. Unicystic ABs only constituted 5.6% of the total sample (3 cases). The duration between radiographs was shorter in the granular cell, follicular and plexiform variants, although not statistically significant ($p = 0.13$). The SGR was analysed between the histopathologic variants, with no statistically significant differences found in all dimensions measured ($p > 0.233$) (Table 4). However, it was interesting to note that the acanthomatous and granular cell variants had higher SGR in most dimensions assessed.

The median proliferation index using Ki-67 IHC of all cases was 6.5%. When excluding the rarer variants of AB, the plexiform and acanthomatous variants showed the highest median proliferation indices, at 12% and 10%, respectively. When assessing the sagittal circumference (or panoramic radiograph circumference), the acanthomatous and plexiform cases had the highest SGR correlated with their higher median proliferation indices. The SGR was examined across categories of Ki-67 proliferation values: low ($\leq 5\%$), intermediate (6%–15%) and high ($> 15\%$), mirroring the approach taken in a study conducted by Ahlem et al. [13] The SGR was comparatively low in the high Ki-67 group, except for the diagonal dimension (Table 5). Overall, no statistically significant correlations were noted between Ki-67 values and SGR ($p > 0.067$). Finally, a stepwise regression analysis of all assessed parameters revealed no correlation with the SGR of ABs. The intra- and inter-examiner reliability for all measurements showed excellent agreement (> 0.954).

4 | Discussion

Ameloblastoma is a frequently studied head and neck tumour due to its relatively high prevalence, presenting as the most common odontogenic neoplasm [1]. The near-equal male-to-female ratio reported in the current study aligns with the literature [14]. ABs have been reported to present earlier in African population groups [5, 15]. Generally, the size of ABs does not differ between age groups [15], and no statistical correlations of SGR could be found with demographic measures [4, 11]. However, larger tumours and faster growth rates have been reported in young males [12, 16]. This was contrary to the current study's findings, whereby more rapid growth was seen in the fourth age quartile. Additionally, females showed higher SGR in the mesial-distal dimension, as well as length expansion and volume. These are noteworthy findings as they ultimately influence the size of the final surgical resection margins.

The radiologic presentation of ABs and some of their unique features have been well described in the literature [5, 17]. In a South African setting, 20% of ABs present with a loss of border demarcation radiologically, likely due to their large size and high prevalence of cortical destruction [15]. In the current study, more than 60% of ABs presented with a loss of border demarcation, with close to 90% exhibiting cortical destruction. Furthermore, the current study noted a statistically significant difference when comparing the SGR to the borders of ABs. ABs with a loss of border demarcation showed faster coronal circumference SGR. These results should be viewed cautiously, as the current study also found that higher SGR was generally seen in cases with well-defined borders.

The radiologic features of ABs evolve over time if left untreated, progressing from well- to poorly-demarcated borders, uni- to multilocular lesions, with increased rates of expansion, cortical thinning and destruction [4]. Furthermore, a statistically significant correlation has been found between larger lesion dimensions and multilocularity [16], with multilocular lesions also showing higher recurrence rates [6, 18]. The influence of multilocularity or size on recurrence rate requires further investigation. The current study found no correlation between lesion locularity and SGR. This is substantiated by studies showing fast growth and high recurrence rates could also be seen in unilocular ABs [12, 19]. Unsurprisingly, the current study found faster SGRs in ABs with severe cortical destruction in some dimensions. More specifically, SGR in length was significantly lower in lesions with cortical thinning compared to those with cortical destruction. The current study found that tooth displacement was seen in significantly faster SGRs in length compared to root resorption. This finding is interesting as faster growth is usually associated with root resorption. Cases with root resorption were noted in older individuals (mean age 35 years) compared to those with tooth displacement (mean age 30 years), emphasising that age did not influence this finding. In this regard, Bi et al. [19] found that the risk of AB recurrence was reduced by 77.5% when associated with root resorption, which may support the current

TABLE 1 | Specific growth rate per year of ameloblastomas between age quartiles.

Age quartile (years)		**Q1 (21.88)**			**Q2 (32.49)**			**Q3 (46.65)**			**Q4 (75.99)**		**p^a**		**Total**		
n (%)		14 (25.9%)			13 (24.1%)			13 (25.9%)			14 (24.1%)						
Duration between radiographs (years)		1.463			1.721			1.145			1.331		0.577	54	0.73		1.79
Total growth between visits (SGR per year) (%)	***n***	**Median**	**IQR**	***n***	**Median**	**IQR**	***n***	**Median**	**IQR**	***n***	**Median**	**IQR**		***n***	**Median**	**IQR**	**CI 95%**	
Diagonal	14	32.98	189.48	13	20.99	47.75	13	21.25	49.74	14	32.04	106.52	0.616	54	26.91	94.3	−133	186
Length	14	48.48	194.01	13	20.01	34.14	13	23.56	68.82	14	42.70	156.27	0.709	54	24.30	127.08	−3	51
Height	14	14.42	83.3	13	38.57	59.48	13	31.13	66.56	14	16.98	128.82	0.378	54	27.06	69.02	15	39
Width	6	20.97	54.41	9	16.92	62.44	7	28.95	133.78	9	22.60	48.54	0.703	31	18.72	60.46	−2	40
Calculated volume	6	47.92	126.39	9	79.53	75.6	7	68.32	424.73	8	105.90	151.81	0.751	30	84.48	121.22	45	124
Length expansion	7	150.48	166.01	9	98.89	255.68	7	43.08	93.42	4	171.96	413.73	0.360	27	98.89	234.85	20	178
Height expansion	11	57.76	598.33	12	31.96	81.23	10	47.21	125.68	10	28.59	629.92	0.819	43	39.01	141.53	11	67
Width expansion	4	55.58	46.89	9	35.39	94.94	7	24.25	77.56	8	83.25	226.56	0.632	28	39.48	81.13	13	66
Calculated expanded volume	4	123.96	184.86	8	195.74	154.25	6	118.07	203.74	4	304.30	342.61	0.630	22	189.53	174.32	107	272
Sagittal circumference	14	50.96	257.6	11	66.16	146.23	12	53.12	161.82	11	44.16	148.47	0.652	48	54.20	147.78	22	87
Coronal circumference	4	−10.79	66.61	8	49.54	114.12	6	43.30	95.6	7	67.06	141.59	0.518	25	42.31	111.85	48	172
Axial circumference	4	15.07	63.59	6	40.61	102.45	4	32.66	74.21	4	101.90	203.05	0.726	18	39.25	81.9	−1	79

Abbreviations: CI, confidence interval; IQR, interquartile range; Q age quartile.
[a]Kruskal–Wallis test.

TABLE 2 | Specific growth rate per year of ameloblastomas between sex.

Sex		Male			Female		p^a		Total		
n (%)		25 (46.3%)			29 (53.7%)						
Duration between radiographs (years)		0.58			0.77		0.768	54	0.73	1.79	
SGR per year (%)	***n***	**Median**	**IQR**	***n***	**Median**	**IQR**		***n***	**Median**	**IQR**	**CI 95%**
Diagonal	25	24.27	62.5	29	30.21	117.41	0.209	54	26.91	94.3	−133 186
Length	25	22.24	56.4	29	73.07	188.00	0.041*	54	24.30	127.08	−3 51
Height	25	31.13	70.35	29	21.89	68.78	0.708	54	27.06	69.02	15 39
Width	14	20.66	47.79	17	16.92	54.41	0.691	31	18.72	60.46	−2 40
Calculated volume	13	68.32	76.03	17	96.68	126.53	0.517	30	84.48	121.22	45 124
Length expansion	11	43.34	119.15	16	150.78	237.81	0.183	27	98.89	234.85	20 178
Height expansion	18	35.36	200.24	25	39.01	122.35	0.902	43	39.01	141.53	11 67
Width expansion	14	42.08	110.76	14	36.08	100.74	0.358	28	39.48	81.13	13 66
Calculated expanded volume	10	174.70	353.84	12	189.54	164.22	0.644	22	189.53	174.32	107 272
Sagittal circumference	21	55.21	148.75	27	53.19	162.55	0.622	48	54.20	147.78	22 87
Coronal circumference	10	66.92	107.68	15	12.58	102.06	0.222	25	42.31	111.85	48 172
Axial circumference	10	57.81	92.07	8	15.07	64.87	0.328	18	39.25	81.9	−1 79

Abbreviations: CI, confidence interval; IQR, interquartile range.
[a]Wilcoxon signed rank test.
*Statistically significant.

study's findings of lower SGR in length in cases presenting with root resorption.

Odukoya et al. [20] found higher growth rates in conventional ABs (0.81cm^3 per month) compared with unicystic ABs (0.17cm^3 per month). The distribution of histopathologic variants in the current study is not a reflection of their true prevalence, but rather influenced by the inclusion and exclusion criteria of the study. For example, the current study only comprised three cases of unicystic AB due to their relative absence of multiple radiographs for assessment of SGR, limiting further observations. Studies have found that desmoplastic ABs have significantly lower growth rates [21] and proliferation indices [9] compared to conventional ABs. In these cases, the desmoplastic stroma likely acts as a barrier, limiting growth [21]. Similar to a systematic literature review by Chae et al. [11], no statistically significant differences were noted in the current study when the SGRs were analysed between the histopathologic variants. However, it was interesting to note that the acanthomatous and granular cell variants had higher SGR in most dimensions assessed. Further studies are necessary in this regard to substantiate these findings. Rarer variants of ABs were included in the study, as they are currently classified under conventional ABs due to similar aetiopathogenic mechanisms and treatment protocols. Although the numbers of these rare variants are limited and prevent detailed comparisons, it improves current knowledge of the growth seen in these variants and provides scope for future studies.

Previous studies have attempted to estimate the growth rate of ABs, with an estimated growth ranging between 40.4%–87.8% or 2.0–9.7cm^3 per year [4, 11, 12, 20]. These studies reported growth over a mean of 9 [11] and 4 years [12] between radiographs, in contrast to the current study, which reported a median duration of less than 2 years between images. The median SGR in the sagittal circumference (panoramic radiograph view) in the current study was 54.20% (mean = 110%), comparable to other studies [12]. High rates of up to 3356.83% have been reported, with follow-up periods of less than a year [11]. Some high values were seen when tumour expansion was compared to the contralateral normal side. In the current study, most lesions showed a positive SGR. However, there were also instances where the tumour decreased in size, with a negative growth rate. This could be explained by cortical destruction resulting in a collapse of the cystic spaces within multilocular ABs, imparting a "pseudomarsupialisation" effect on the tumour (Figure 2). This was supported by cases showing a loss of border demarcation and cortical destruction having a lower SGR. This decrease was only noted in specific dimensions measured; for example, if the lesion had buccal perforation and resulted in a collapse of cystic space, the buccal-lingual (width and coronal circumference) measurement may decrease. However, this might still be accompanied by an increase in length, emphasising the importance of assessing the lesion in multiple dimensions.

Ki-67 proliferation indices indicate tumour aggressiveness, with significantly higher values reported in recurrent ABs and those with shorter disease-free survival [13, 22, 23]. The Ki-67 proliferation index also differs between the histopathologic variants of ABs, with some studies finding higher values in follicular ABs [8, 9, 24] and others finding higher values in plexiform ABs [25–28]. However, no statistical correlations were found when comparing age, sex, site, size, or histopathologic variant of ABs

TABLE 3 | Specific growth rate per year of ameloblastomas between radiologic features.

Radiologic features	Well-defined borders	Loss of border demarcation	p^a	Unilocular	Multilocular	p^a	Reactive bone	p^a	Cortical thinning	p^a	Cortical destruction			p^a	Tooth impaction	p^a	Tooth displacement	Root resorption	p^a
											Mild	Moderate	Severe						
n (%)	20 (37%)	34 (63%)		10 (19%)	44 (81%)		17 (31%)		5 (9%)		14 (26%)	17 (31%)	16 (30%)		12 (22%)		5 (9%)	33 (61%)	
SGR per year (%)																			
Diagonal	29.4	24.8	0.20	40.7	26.5	0.98	24.3	0.64	11.3	0.14	33.0	31.0	24.8	1.00	21.2	0.79	196.9	28.6	0.06
Length	21.3	33.0	0.18	14.0	29.0	0.33	20.4	0.42	5.7	0.02*	47.7	24.7	36.2	0.65	23.6	0.99	285.2	23.6	0.002*
Height	30.6	24.2	0.67	25.9	31.1	0.67	32.3	0.80	4.5	0.50	30.6	24.2	31.1	0.93	39.6	0.63	79.2	23.0	0.43
Width	29.3	16.9	0.97	22.6	18.7	0.60	18.7	1.00	−1.4	0.23	−2.4	16.1	46.8	0.08	9.0	0.51	−16.5	34.3	0.41
Calculated volume	92.1	66.6	0.86	96.5	84.5	0.67	79.5	0.65	3.0	0.14	43.0	65.0	94.9	0.59	77.2	0.84	−8.6	89.4	0.42
Length expansion	150.8	43.3	0.18	209.1	51.9	0.24	51.9	0.21	27.9	0.52	150.5	20.0	109.0	0.25	98.9	0.58	155.4	113.4	0.57
Height expansion	68.6	34.2	0.25	36.3	39.0	1.00	40.0	0.92	−11.1	0.20	68.6	31.5	41.0	0.69	51.7	0.52	−1.1	34.4	0.19
Width expansion	17.0	44.2	0.21	29.9	39.5	0.47	37.3	0.94	−8.9	0.15	9.1	24.2	64.4	0.96	35.6	0.79	−27.4	46.9	0.43
Calculated expanded volume	207.6	138.4	0.50	233.8	183.8	0.23	121.4	0.34	0.5	0.13	137.7	83.7	206.4	0.36	195.1	0.82	222.5	206.4	0.82
Sagittal circumference	59.6	43.2	0.98	20.2	55.2	0.50	53.2	0.70	4.2	0.13	66.7	59.6	34.2	0.77	3.8	0.54	81.0	64.3	0.64
Coronal circumference	−6.1	55.7	0.04*	−11.3	56.1	0.10	48.9	0.64	0.6	0.27	−20.2	−6.1	89.5	0.01	25.3	0.31	124.4	64.1	0.53
Axial circumference	47.5	33.7	0.35	49.4	39.2	0.78	4.6	0.19	−2.8	0.50	15.1	−4.3	75.4	0.22	72.8	0.75	−15.2	68.1	0.17

Abbreviations: CI, confidence interval; IQR, interquartile range.
[a]Dunn's pairwise comparison using rank sums with Bonferroni correction.
*Statistically significant.

TABLE 4 | Specific growth rate per year of ameloblastomas between histopathological variants.

Variants	Uni			Fo			Pl			AA			Gr			KA			De	Ba	p^a
n (%)	3 (5.6%)			18 (33.3%)			5 (9.3%)			17 (31.5%)			6 (11.1%)			3 (5.6%)			1 (1.9%)	1 (1.9%)	
Duration between radiographs (years)	1.92			0.46			0.77			1.55			0.11			1.9			0.58	1.45	0.125
SGR per year (%)	***n***	**Median**	**IQR**	***n***	**Median**	**IQR**	***n***	**Median**	**IQR**	***n***	**Median**	**IQR**	***n***	**Median**	**IQR**	***n***	**Median**	**IQR**	**Median**		***p*** [a]
Diagonal	3	15.12	152.09	18	46.39	119.68	5	25.24	14.14	17	50	118.53	6	5.22	44.42	3	24.39	664.11	24.27	−4.47	0.26
Length	3	18.44	270.28	18	42.7	225.69	5	18.44	8.69	17	23.88	194.01	6	45.09	106.95	3	17.93	970.66	32.49	5.74	0.607
Height	3	29.96	294.73	18	20.64	67.37	5	14.49	25.15	17	38.57	78.6	6	35.05	132.1	3	16.86	337.03	31.13	−2.42	0.966
Width	2	22.56	34.77	11	14.89	93.35	3	53.47	53.38	9	30.08	54.41	2	181.7	138.47	2	−5.29	22.45	28.95	−7.96	0.263
Calculated volume	2	67.64	113.99	10	88.54	181.48	3	68.32	82.02	9	89.42	118.68	2	291.9	394.07	2	5.13	27.42	92.57	−4.63	0.521
Length expansion	1	150.48	0	9	98.89	243.01	5	14.64	50.9	7	258.07	313.09	2	69.57	99.22	1	−11.9	0	43.08	27.91	0.233
Height expansion	1	72.38	0	17	15.4	89.91	5	57.76	90.14	10	46.83	635.03	5	18.18	36.48	3	650.13	624.75	40.98	−11.08	0.36
Width expansion	2	31.41	65.79	10	27.4	166.5	3	67.58	59.04	7	46.85	50.06	2	66.64	446.97	2	−6.63	41.45	37.32	−16.29	0.728
Calculated expanded volume	1	233.83	0	8	203.17	284.24	3	138.37	169.78	5	206.38	12.39	2	218.81	389.07	1	−31.81	0	121.38	0.54	0.523
Sagittal circumference	3	13.28	206.54	14	36.88	172.03	3	53.19	32.57	17	70.62	101.18	6	53.12	148.47	3	33.17	133.5	34.15	−4.39	0.901
Coronal circumference	2	−11.28	37.08	11	42.31	140.61	3	44.3	78.96	5	67.06	16.19	1	−114.5	0	1	−10.57	0	89.55	−6.05	0.447
Axial circumference	1	25.55	0	6	39.25	83.75	2	80.52	14.52	6	62.57	15.39	0	na	na	2	−9.48	10.38	na	−2.78	0.475

Abbreviations: AA, acanthomatous; Ba, basaloid; De, desmoplastic; Fo, follicular; Gr, granular cell; IQR, interquartile range; KA, keratoameloblastoma; Pl, plexiform; Uni, unicystic.
[a]Dunn's pairwise comparison using rank sums with Bonferroni correction.

TABLE 5 | Specific growth rate per year of ameloblastomas between low, intermediate and high Ki-67 categories.

Ki-67	Low (≤5%)			Intermediate (6%–15%)			High (>15%)			p^a	Total			
n (%)	27 (50%)			13 (24%)			14 (26%)							
Duration between radiographs (years)	0.56			1.11			0.73			0.840	54	0.73	1.79	
SGR per year (%)	***n***	**Median**	**IQR**	***n***	**Median**	**IQR**	***n***	**Median**	**IQR**		***n***	**Median**	**IQR**	**CI 95%**	
Diagonal	27	21.25	67.68	13	30.21	119.54	14	33.37	130.29	0.453	54	26.91	94.3	−133	186
Length	27	33.40	151.13	13	20.29	178.00	14	22.16	148.68	0.703	54	24.30	127.08	−3	51
Height	27	29.96	69.12	13	37.11	105.41	14	16.87	92.17	0.750	54	27.06	69.02	15	39
Width	17	39.95	67.66	8	14.47	47.76	6	−0.50	82.78	0.289	31	18.72	60.46	−2	40
Calculated volume	16	104.40	80.26	8	65.10	108.82	6	17.39	204.16	0.067	30	84.48	121.22	45	124
Length expansion	13	119.18	245.19	8	120.08	570.67	6	64.80	93.52	0.075	27	98.89	234.85	20	178
Height expansion	20	40.75	115.13	11	57.76	648.07	12	31.47	121.23	0.746	43	39.01	141.53	11	67
Width expansion	14	58.70	131.09	8	24.75	69.79	6	38.70	266.62	0.533	28	39.48	81.13	13	66
Calculated expanded volume	11	207.64	298.60	6	200.81	193.24	5	60.16	300.68	0.384	22	189.53	174.32	107	272
Sagittal circumference	23	70.62	162.55	11	53.19	236.95	14	46.45	93.06	0.560	48	54.20	147.78	22	87
Coronal circumference	14	43.30	170.62	6	61.55	95.68	5	12.58	106.42	0.685	25	42.31	111.85	48	172
Axial circumference	7	68.09	140.38	7	44.81	81.90	4	9.51	232.43	0.701	18	39.25	81.9	−1	79

Abbreviations: CI, confidence interval; IQR, interquartile range.
[a]Kruskal–Wallis test.

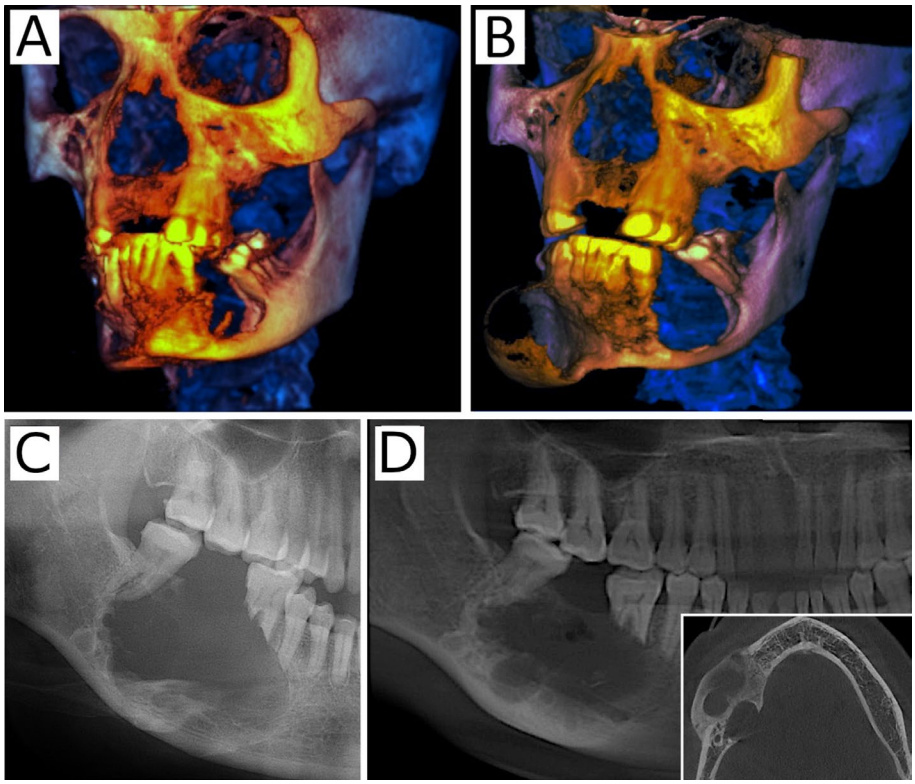

FIGURE 2 | Ameloblastoma showing growth between the initial (A) and follow-up (B) radiographs after 15 months. In contrast, an ameloblastoma with a decrease in size between the initial (C) and follow-up (D) radiographs. On the axial CBCT image (insert), cortical destruction and reactive bony thickening can be seen.

and Ki-67 values [13]. A study by Li et al. [29] found a statistically significant correlation between high Ki-67 values and loss of border demarcation, along with higher recurrence rates [29]. Conversely, Sandra et al. [8] found no association between radiologic features and the proliferation indices, concluding that the proliferation rate cannot predict the radiologic presentation of ABs. In the current study, higher Ki-67 values were seen in cases with lower SGR, apart from the diagonal and sagittal circumference measurements. Theoretically, the opposite findings were expected. However, if one considers the faster growth resulting in cortical destruction, leading to a pseudomarsupialisation of cystic spaces and, hence, a decrease in tumour size, it will impact the growth rate.

The limitations of this study include that initial and follow-up CBCT images were not available for all patients, resulting in comparisons between different imaging modalities. Using a percentage growth rate between two calibrated images mitigated this limitation. In some cases, the whole lesion could not be measured in one view, which resulted in excluding that particular measurement. Cases with severe cortical destruction resulted in difficulty in determining the tumour margin.

Delays in treatment, attributed to various factors, are reported in the literature [11], especially in developing countries. Financial/travel/healthcare constraints, fear, lack of communication and other factors may result in a loss of patient follow-up or treatment interruption [11]. This is an unfortunate reality that is often seen in developing countries. In the current study setting, patients are lost to follow-up for various reasons and, upon their return, require re-evaluation of the tumour, resulting in multiple pre-treatment radiographs. The strength of this study, measuring the SGR of 54 cases of AB, lies in its large sample compared to the systematic review by Chae et al. ($n = 16$) [11], and another similar study by Mariz et al. ($n = 12$) [12]. The current study also assessed the SGR of ABs in multiple dimensions.

5 | Conclusion

In conclusion, this study found significant findings regarding coronal dimensions, supporting the notion of buccal-lingual growth/expansion for which ABs are known. Although no clinical or histopathologic signs predict fast-growing ABs, future studies should assess for associations with the various gene mutations that ultimately drive the pathogenesis of these neoplasms.

Author Contributions

Chané Smit: conceptualisation, data curation, formal analysis, investigation, methodology, writing – original draft, writing – review and editing. **Liam Robinson:** data curation, investigation, methodology, writing – review and editing. **Marlene B. van Heerden:** data curation, investigation, methodology, writing – review and editing. **Pieter W. Meyer:** data curation, investigation, methodology, writing – review and editing. **Felipe P. Fonseca:** investigation, project administration, supervision, writing – review and editing. **Willie F. P. van Heerden:** investigation, project administration, supervision, writing – review and editing. **André Uys:** investigation, project administration, supervision, writing – review and editing.

Ethics Statement

This study was approved by the University of Pretoria, Faculty of Health Sciences Research Ethics Committee (Reference no.: 723/2022, approval date: 19/01/2023, renewal date: 18/01/2024). All procedures followed the ethical standards of the Helsinki Declaration of 1975, as revised in 2008. This article does not contain any studies with human or animal subjects performed by any of the authors.

Conflicts of Interest

The authors declare no conflicts of interest.

Data Availability Statement

The data of the current study is summarised in the figures and tables. Access to raw data is subject to approval by the University of Pretoria, Faculty of Health Sciences Research Ethics Committee.

Peer Review

The peer review history for this article is available at https://www.webofscience.com/api/gateway/wos/peer-review/10.1111/jop.13611.

References

1. WHO Classification of Tumours Editorial Board, *Head and Neck Tumours*, 5th ed. (Lyon (France): International Agency for Research on Cancer, 2024).

2. L. Robinson, C. Smit, F. P. Fonseca, et al., "Keratoameloblastoma: A Report of Seven New Cases and Review of Literature," *Head and Neck Pathology* 16, no. 4 (2022): 1103–1113, https://doi.org/10.1007/s12105-022-01470-5.

3. D. C. Brown and K. C. Gatter, "Ki67 Protein: The Immaculate Deception?," *Histopathology* 40, no. 1 (2002): 2–11, https://doi.org/10.1046/j.1365-2559.2002.01343.x.

4. L. Merbold, C. Smit, J. Ker-Fox, and A. Uys, "The Radiologic Progression of Ameloblastomas," *South African Journal of Radiology* 27, no. 1 (2023): 1–8, https://doi.org/10.4102/sajr.v27i1.2668.

5. C. Smit, L. Robinson, J. Ker-Fox, F. P. Fonseca, W. F. P. van Heerden, and A. Uys, "Clinicoradiologic Features of Ameloblastomas: A Single-Centre Study of 155 Cases," *Journal of Oral Pathology & Medicine* 53, no. 2 (2024): 133–141, https://doi.org/10.1111/jop.13510.

6. S. Ueno, K. Mushimoto, and R. Shirasu, "Prognostic Evaluation of Ameloblastoma Based on Histologic and Radiographic Typing," *Journal of Oral and Maxillofacial Surgery* 47, no. 1 (1989): 11–15, https://doi.org/10.1016/0278-2391(89)90116-X.

7. C. Smit, L. Robinson, M. B. van Heerden, et al., "A Radiologic-Pathologic Study of the Histopathologic Variants of Ameloblastomas and Their Proliferation Indices," *Oral Surgery, Oral Medicine, Oral Pathology, Oral Radiology* 138 (2024): 403–413, https://doi.org/10.1016/j.oooo.2024.03.007.

8. F. Sandra, T. Mitsuyasu, N. Nakamura, Y. Shiratsuchi, and M. Ohishi, "Immunohistochemical Evaluation of PCNA and Ki-67 in Ameloblastoma," *Oral Oncology* 37, no. 2 (2001): 193–198, https://doi.org/10.1016/S1368-8375(00)00079-8.

9. R. Bologna-Molina, A. Mosqueda-Taylor, N. Molina-Frechero, A. Mori-Estevez, and G. Sanchez-Acuna, "Comparison of the Value of PCNA and Ki-67 as Markers of Cell Proliferation in Ameloblastic Tumors," *Medicina Oral, Patología Oral y Cirugía Bucal* 18, no. 2 (2013): 174–179, https://doi.org/10.4317/medoral.18573.

10. E. Mehrara, E. Forssell-Aronsson, and P. Bernhardt, "Objective Assessment of Tumour Response to Therapy Based on Tumour Growth Kinetics," *British Journal of Cancer* 105, no. 5 (2011): 682–686, https://doi.org/10.1038/bjc.2011.276.

11. M. P. Chae, N. R. Smoll, D. J. Hunter-Smith, and W. M. Rozen, "Establishing the Natural History and Growth Rate of Ameloblastoma With Implications for Management: Systematic Review and Meta-Analysis," *PLoS One* 10, no. 2 (2015): e0117241, https://doi.org/10.1371/journal.pone.0117241.

12. B. Mariz, B. Andrade, M. Agostini, et al., "Radiographic Estimation of the Growth Rate of Initially Underdiagnosed Ameloblastomas," *Medicina Oral, Patología Oral y Cirugía Bucal* 24, no. 4 (2019): 468–472, https://doi.org/10.4317/medoral.23003.

13. B. Ahlem, A. Wided, L. Amani, Z. Nadia, A. Amira, and F. Faten, "Study of Ki67 and CD10 Expression as Predictive Factors of Recurrence of Ameloblastoma," *European Annals of Otorhinolaryngology, Head and Neck Diseases* 132, no. 5 (2015): 275–279, https://doi.org/10.1016/j.anorl.2015.08.016.

14. F. N. Hendra, E. M. Van Cann, M. N. Helder, et al., "Global Incidence and Profile of Ameloblastoma: A Systematic Review and Meta-Analysis," *Oral Diseases* 26, no. 1 (2020): 12–21, https://doi.org/10.1111/odi.13031.

15. S. Ranchod, F. Titinchi, N. Behardien, and J. Morkel, "Ameloblastoma of the Mandible: Analysis of Radiographic and Histopathological Features," *Journal of Oral Medicine and Oral Surgery* 27, no. 1 (2021): 6, https://doi.org/10.1051/mbcb/2020051.

16. A.-F. Safi, M. Kauke, M. Timmer, et al., "Does Volumetric Measurement Serve as an Imaging Biomarker for Tumor Aggressiveness of Ameloblastomas?," *Oral Oncology* 78 (2018): 16–24, https://doi.org/10.1016/j.oraloncology.2018.01.002.

17. D. MacDonald-Jankowski, R. Yeung, K. Lee, and T. Li, "Ameloblastoma in the Hong Kong Chinese. Part 2: Systematic Review and Radiological Presentation," *Dentomaxillofacial Radiology* 33, no. 3 (2004): 141–151, https://doi.org/10.1259/dmfr/28001874.

18. A. Rodriguez-Archilla and C. Barragan-Muñoz, "Influence of Ki-67 and Proliferating Cell Nuclear Antigen Expression on the Biological Behavior of Ameloblastomas," *Dentistry and Medical Research* 6, no. 2 (2018): 27, https://doi.org/10.4103/dmr.dmr_22_18.

19. L. Bi, D. Wei, D. Hong, et al., "A Retrospective Study of 158 Cases on the Risk Factors for Recurrence in Ameloblastoma," *International Journal of Medical Sciences* 18, no. 14 (2021): 3326–3332, https://doi.org/10.7150/ijms.61500.

20. O. Odukoya and O. A. Effiom, "Clinicopathological Study of 100 Nigerian Cases of Ameloblastoma," *Nigerian Postgraduate Medical Journal* 15, no. 1 (2008): 1–5.

21. O. A. Effiom and O. Odukoya, "Desmoplastic Ameloblastoma: Analysis of 17 Nigerian Cases," *Oral Surgery, Oral Medicine, Oral Pathology, Oral Radiology, and Endodontology* 111, no. 1 (2011): e27–e31, https://doi.org/10.1016/j.tripleo.2010.06.021.

22. M. Migaldi, G. Sartori, G. Rossi, A. Cittadini, and A. Sgambato, "Tumor Cell Proliferation and Microsatellite Alterations in Human Ameloblastoma," *Oral Oncology* 44, no. 1 (2008): 50–60, https://doi.org/10.1016/j.oraloncology.2006.12.004.

23. A. Abdel-Aziz and M. M. Amin, "EGFR, CD10 and Proliferation Marker Ki67 Expression in Ameloblastoma: Possible Role in Local Recurrence," *Diagnostic Pathology* 7, no. 1 (2012): 14, https://doi.org/10.1186/1746-1596-7-14.

24. M. N. Ong'uti, A. T. Cruchley, G. L. Howells, and D. M. Williams, "Ki-67 Antigen in Ameloblastomas: Correlation With Clinical and Histological Parameters in 54 Cases From Kenya," *International Journal of Oral and Maxillofacial Surgery* 26, no. 5 (1997): 376–379, https://doi.org/10.1016/S0901-5027(97)80801-6.

25. M. Jabbarzadeh, M. R. Hamblin, F. Pournaghi-Azar, M. Vakili Saatloo, M. Kouhsoltani, and N. Vahed, "Ki-67 Expression as a Diagnostic Biomarker in Odontogenic Cysts and Tumors: A Systematic Review and Meta-Analysis," *Journal of Dental Research, Dental Clinics, Dental Prospects* 15, no. 1 (2021): 66–75, https://doi.org/10.34172/joddd.2021.012.

26. K. Gupta, T. P. Chaturvedi, J. Gupta, and R. Agrawal, "Cell Proliferation Proteins and Aggressiveness of Histological Variants of Ameloblastoma and Keratocystic Odontogenic Tumor," *Biotechnic & Histochemistry* 94, no. 5 (2019): 348–351, https://doi.org/10.1080/10520295.2019.1571226.

27. Y. Koizumi, A. Kauzman, H. Okada, K. Kuyama, R. J. McComb, and H. Yamamoto, "Assessment of Proliferative Activity and Angiogenesis in Ameloblastoma: A Comparison Based on Patient Age," *International Journal of Oral-Medical Sciences* 3, no. 1 (2004): 25–33, https://doi.org/10.5466/ijoms.3.25.

28. T. Hirayama, T. Hamada, K. Hasui, I. Semba, F. Murata, and K. Sugihara, "Immunohistochemical Analysis of Cell Proliferation and Suppression of Ameloblastoma With Special Reference to Plexiform and Follicular Ameloblastoma," *Acta Histochemica et Cytochemica* 37, no. 6 (2004): 391–398, https://doi.org/10.1267/ahc.37.391.

29. Y. Li, B. Han, and L.-J. Li, "Prognostic and Proliferative Evaluation of Ameloblastoma Based on Radiographic Boundary," *International Journal of Oral Science* 4, no. 1 (2012): 30–33, https://doi.org/10.1038/ijos.2012.8.